Exclusive Processes in Leptoproduction at COMPASS

Andrzej Sandacz[1]
on behalf of the COMPASS Collaboration

[1]Sołtan Institute for Nuclear Studies, ul. Hoża 69, 00681 Warsaw, Poland

DOI: will be assigned

Selected topics on exclusive ρ^0 production from the COMPASS experiment are discussed. They include the transverse target spin asymmetry, the longitudinal double-spin asymmetry and the spin density matrix elements. Future plans for the GPD studies at COMPASS and results from a DVCS test run are also presented.

1 Introduction

Exclusive processes in electro- and muoproduction have played an important role in studying strong interactions and gained a renewed interest, as they can give access to Generalized Parton Distributions (GPDs) and thus to a wealth of information on the nucleon structure. A study of Hard Exclusive Meson Production and Deeply Virtual Compton Scattering (DVCS) is a part of the COMPASS physics program. In addition, COMPASS provides also large statistics data for meson production in the non-perturbative region at low Q^2.

The recent results from COMPASS on the transverse target spin asymmetries for ρ^0 production off polarised protons and deuterons will be discussed in Sect. 3. Other advanced analyses are those of the longitudinal double spin asymmetry (Sect. 4), of the spin density matrix elements (Sect. 5), and of Q^2- and W-dependence of unpolarised cross sections, separated σ_L and σ_T cross sections and the $t-$ slopes of cross sections $\mathrm{d}\sigma/\mathrm{d}t$. Experimental tests of feasibility to isolate exclusive single photon events have just started at COMPASS and the results will be briefly discussed in Sect. 6.

2 COMPASS experimental set-up

A high intensity positive muon beam from the CERN SPS, of 160 GeV/c momentum and -76% average polarisation, impinges on a large solid-state polarised target. The polarisable material is either ^{6}LiD with 50% deuteron polarisation or NH_3 with 90% proton polarisation. Both protons and deuterons could be polarised either longitudinally or transversely with respect to the beam direction. The targets contain either two or three separate cells with polarisable material, placed one after another along the beam. The beam traverses 120 cm of the total length of polarised material. Polarisation directions in the alternate cell are opposite and are periodically reversed.

The COMPASS detector consists of two high resolution magnetic spectrometers equipped with tracking detectors, electromagnetic and hadronic calorimetry and muon identification. The first, large angle spectrometer is equipped with the RICH detector. A detailed description of the COMPASS apparatus can be found in [1].

3 Transverse target spin asymmetries for ρ^0 production

3.1 Theoretical motivation

It was pointed out that vector meson production on a transversely polarised target is sensitive to the nucleon helicity-flip GPD E [2, 3]. This GPD offers unique views on the orbital angular momentum carried by partons in the proton [4] and on the correlation between polarisation and spatial distribution of partons [5].

The reference [6] provides a detailed framework to our study. The cross section of the reaction $\mu + N \to \mu' + \rho^0 + N'$ on a transversely polarised nucleon is a function of the kinematic variables x_B, Q^2, t, ϕ and ϕ_S. Here ϕ is the azimuthal angle between the lepton plane and the hadron plane and ϕ_S is the azimuthal angle of the the target spin vector S_T w.r.t. the virtual photon direction. An observable which allows access to the GPD E is the transverse target spin asymmetry w.r.t. virtual photon direction defined as

$$A_{UT}(\phi, \phi_S) = \frac{1}{S_T} \cdot \frac{d\sigma(\phi, \phi_S) - d\sigma(\phi, \phi_S + \pi)}{d\sigma(\phi, \phi_S) + d\sigma(\phi, \phi_S + \pi)} \,. \tag{1}$$

The modulation of asymmetry as a function of $\sin(\phi - \phi_{\rm s})$ in deep inelastic kinematics region can be expressed as

$$A_{UT}^{\sin(\phi-\phi_{\rm s})}(\phi, \phi_S) \quad \propto \quad \frac{\mathrm{Im}(\sigma_{++}^{+-} + \epsilon\, \sigma_{00}^{+-})}{\frac{1}{2}(\sigma_{++}^{++} + \sigma_{++}^{--}) + \epsilon\, \sigma_{00}^{++}} \,. \tag{2}$$

The notation for the cross sections and interference terms is that of Ref. [6], with the lower indices referring to the helicities of the virtual photon and the upper ones to the helicities of the target proton, and ϵ is the virtual photon polarisation parameter. The only leading-twist observables are the longitudinal cross section σ_{00}^{++} and the interference term σ_{00}^{+-}. They can be written as:

$$\frac{1}{\Gamma'}\frac{d\sigma_{00}^{++}}{dt} = (1-\xi^2)|\mathcal{H}_M|^2 - (\xi^2 + \frac{t}{4M_p^2})|\mathcal{E}_M|^2 - 2\xi^2 \mathrm{Re}(\mathcal{E}_{\rm M}^* \mathcal{H}_{\rm M}), \tag{3}$$

$$\frac{1}{\Gamma'}\frac{d\sigma_{00}^{+-}}{dt} = -\sqrt{1-\xi^2}\frac{\sqrt{t_0 - t}}{M_p}\mathrm{Im}(\mathcal{E}_{\rm M}^* \mathcal{H}_{\rm M}) \,, \tag{4}$$

where $\Gamma' = \alpha_{em}/Q^6 \times x_B^2/(1-x_B)$, the skewedness variable is $\xi = x_B/(2-x_B)$ and the minimal four-momentum transfer is $t_0 = -4\xi^2 M_p^2/(1-\xi^2)$. The quantities $\mathcal{H}_M$ and $\mathcal{E}_M$ are weighted sums of integrals over the GPD $H^{q,g}$ and $E^{q,g}$ respectively. The weights depend on the contributions of quarks of various flavours and of gluons to the production of meson M (ρ^0 in present analysis).

3.2 Event sample

The results presented in Sect. 3 were obtained using the full sets of data with transversely polarised protons from the NH_3 target taken in 2007, and with transversely polarised deuterons from the ^{6}LiD target taken in 2002-2004. As an example, the selection of the sample of incoherent exclusive ρ^0 production will be described here for the 2007 data.

In order for an event to be accepted, it was required to originate inside the target, have reconstructed beam and scattered muon tracks and have only two additional tracks, which correspond to charged pions from the decay of ρ^0. A cut on the invariant mass of two pions, $0.47 < m_{\pi\pi} < 1.07\,\mathrm{GeV}/c^2$, selects the ρ^0. As the slow recoil target particles are not detected, in order to select exclusive events we use the cut on the missing energy, $-2.5 < E_{miss} < 2.5$ GeV, on the transverse momentum of ρ^0 with respect to the direction of virtual photon, $p_t^2 < 0.5\,(\mathrm{GeV/c})^2$, and on the ρ^0 energy, $E_\rho > 15$ GeV. Here $E_{miss} = (M_X^2 - M_p^2)/2M_p$, where M_X is the missing mass of an unobserved recoiling system and M_p is the proton mass. Coherent interactions on the nitrogen and other nuclei in the target are removed by a cut $p_t^2 > 0.05\,(\mathrm{GeV/c})^2$. To obtain a final data sample of events in the deep inelastic region, the negative four-momentum squared of the virtual photon is restricted to $Q^2 > 1.0\,(\mathrm{GeV}/c)^2$, while the region of hadron resonances is excluded by applying a cut on the total energy in the $\gamma^* N$ center of mass system, $W > 5.0$ GeV. Another cut is applied on the variable y, $0.1 < y < 0.9$, in order to remove events with large radiative corrections (large y) or poorly reconstructed kinematics (low y).

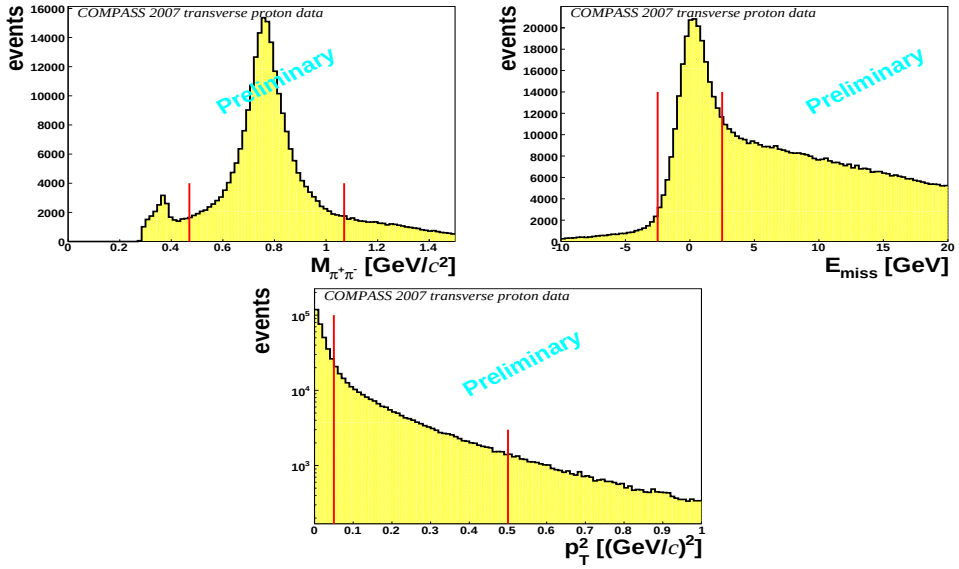

Figure 1: Distributions of $M_{\pi\pi}$ (top left), E_{miss} (top right) and p_t^2 (bottom) for the exclusive sample. The arrows show cuts imposed on each variable to define the final sample.

The distributions of $m_{\pi\pi}$, E_{miss} and p_t^2 are shown in Fig. 1. Each plot is obtained applying all cuts except those corresponding to the displayed variable. On the left top panel of Fig. 1 a clear peak of the ρ^0 resonance is visible on the top of the small contribution of background

of the non-resonant $\pi\pi$ pairs. A small bump below 0.4 GeV/c^2 is due to assignment of the charged pion mass to the kaons from decays of ϕ mesons.

On the right top panel of the figure the peak at $E_{miss} \approx 0$ is the signal of exclusive ρ^0 production. The width of the peak, $\sigma \approx 1.1$ GeV, is due to the spectrometer resolution. Non-exclusive events, where in addition to the recoil nucleon other undetected hadrons are produced, appear at $E_{miss} > 0$.

The p_t^2 distribution shown on the bottom panel of the figure indicates a contribution from coherent production on target nuclei at small p_t^2 values. A three exponential functions fit to this distribution was performed, which indicates also a contribution of non-exclusive background increasing with p_t^2. Therefore to select the sample of exclusive incoherent ρ^0 production, the aforementioned p_t^2 cuts, indicated by arrows, were applied.

After all selections the final sample for incoherent exclusive ρ^0 production consists of about 230 000 events.

3.3 Extraction of the transverse target spin asymmetry

The numbers of events as a function of the angle $\eta = \phi - \phi_S$ is given by

$$N(\eta) = Fn\sigma a(\eta)(1 + \epsilon sin(\eta)) \,, \tag{5}$$

where F is the muon flux, n the number of target particles, σ the spin averaged cross-section, $a(\eta)$ the product of angular acceptance and efficiency of the apparatus and ϵ is the raw asymmetry. It should be taken into account that $a(\eta)$ is not known precisely enough and it is different for the different target cells. To minimize acceptance effects, the double ratio method was chosen. The double ratio (DR) is calculated for 10 angular bins in η

$$F(\eta) = \frac{(N_u^{\uparrow}(\eta) + N_d^{\uparrow}(\eta)) \cdot N_c^{\uparrow}(\eta)}{(N_u^{\downarrow}(\eta) + N_d^{\downarrow}(\eta)) \cdot N_c^{\downarrow}(\eta)} = \frac{(1 + \epsilon \cdot sin(\eta))^2}{(1 - \epsilon \cdot sin(\eta))^2} \,, \tag{6}$$

where $\uparrow(\downarrow)$ indicate up/down target polarisation and $u/c/d$ refer to the upstream/central/downstream target cells. This relation is obtained with a plausible assumption that the ratio of combinations of acceptances for various cells is the same before and after the polarisation reversal

$$\frac{a_u^-(\eta) + a_d^-(\eta)}{a_c^+(\eta)} = \frac{a_u^+(\eta) + a_d^+(\eta)}{a_c^-(\eta)} \,. \tag{7}$$

The raw asymmetry ϵ is determined from a fit to the DR dependence on the angle $\eta = \phi - \phi_S$. The transverse target asymmetry is extracted using expression

$$A_{UT}^{\sin(\phi-\phi_s)} = \frac{\epsilon}{f \cdot \langle P_T \rangle} \,, \tag{8}$$

where $f \simeq 0.14$ is the mean value of the dilution factor for the polarised target and $\langle P_T \rangle \simeq 0.9$ is the mean value of the proton polarisation.

3.4 Results for $A_{UT}^{\sin(\phi-\phi_s)}$

The transverse target spin asymmetry $A_{UT}^{\sin(\phi-\phi_s)}$ for the proton is shown in Fig. 2 as a function of Q^2, x_B and p_t^2. The average values of kinematic variables for this sample are $\langle Q^2 \rangle =$

2.2 $(\mathrm{GeV}/c)^2$, $\langle x_{Bj} \rangle = 0.4$ and $\langle p_t^2 \rangle = 0.18\,(\mathrm{GeV}/c)^2$. The errors shown are statistical ones. Preliminary estimates of systematic errors indicate that they are smaller than the statistical ones. The asymmetry is consistent with zero within the statistical errors.

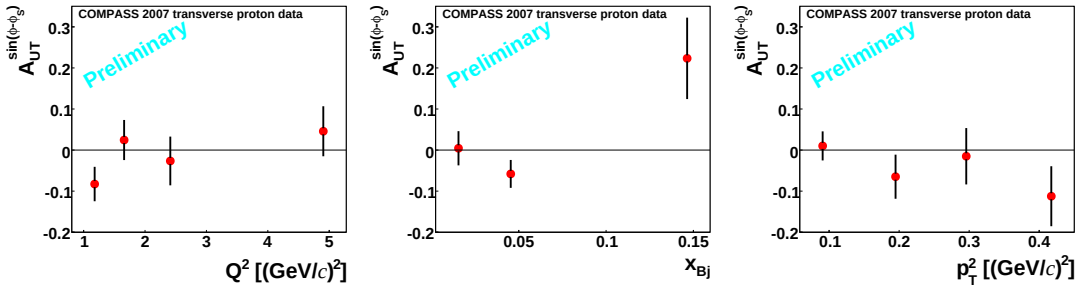

Figure 2: $A_{UT}^{\sin(\phi-\phi_s)}$ for the proton target as a function of Q^2, x_B and p_t^2.

A similar analysis of $A_{UT}^{\sin(\phi-\phi_s)}$ for the deuteron was done using the data taken in 2002-2004 with transversely polarised ^{6}LiD target. The selections for the exclusive ρ^0 sample were similar to these for the NH_3 data, except the coherent and incoherent contributions to the exclusive production on the deuteron were not separated. The applied cut on p_t^2 was $0.01 < p_t^2 < 0.5\,(\mathrm{GeV}/c)^2$.The number of events for this sample is about 270 000. The transverse target spin asymmetry for the deuteron is shown in Fig. 3 as a function of Q^2, x_B and p_t. (Note the difference in the transverse momentum scales in Figs 2 and 3.) The asymmetry for the deuteron is consistent with zero as well.

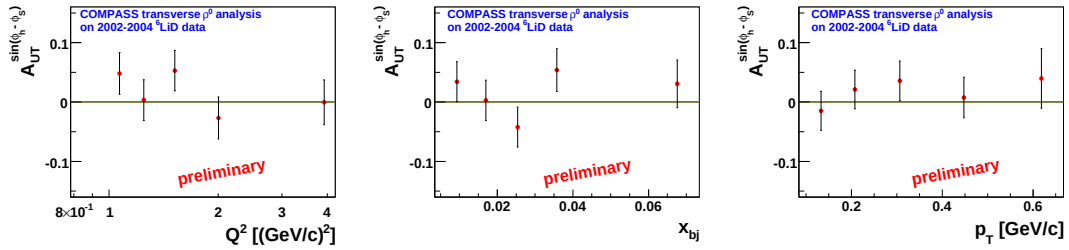

Figure 3: $A_{UT}^{\sin(\phi-\phi_s)}$ for the deuteron target as a function of Q^2, x_B and p_t.

A further analysis is in progress to separate the leading term σ_{00}^{+-} and the subleading term σ_{++}^{+-} (cf. Eq. 2), both for protons and deuterons, to separate coherent and incoherent contributions for the deuterons and to estimate effects of the non-exclusive background on the systematic errors.

The asymmetry $A_{UT}^{\sin(\phi-\phi_s)}$ for ρ^0 for the proton target was first obtained by the HERMES collaboration [7]. The HERMES results are consistent with zero within statistical errors, which are of a comparable magnitude as for COMPASS. The longitudinal and transverse separation has also been accomplished by HERMES.

Theoretical predictions for $A_{UT}^{\sin(\phi-\phi_s)}$ for ρ^0 have been done by Goloskokov and Kroll [8,

9]. The predicted values for asymmetry on the proton is about -0.02 for ρ^0 production, but significantly higher, about -0.10, for ω production.

4 Double spin asymmetry in exclusive ρ^0 production

Here we discuss the longitudinal double-spin asymmetry $A_1^\rho = (\sigma_{1/2} - \sigma_{3/2})/(\sigma_{1/2} + \sigma_{3/2})$ for incoherent ρ^0 production on polarized deuterons. The cross sections $\sigma_{1/2}$ and $\sigma_{3/2}$ refer to the cases when the absolute value of the total photon-nucleon angular momentum component along the virtual photon axis is 1/2 or 3/2, respectively. In the Regge approach the longitudinal double spin asymmetry A_1^ρ can arise due to the interference of amplitudes for exchange in the t-channel of Reggeons with natural parity (Pomeron, ρ, ω, f, A_2) with amplitudes for Reggeons with unnatural parity (π, A_1). For large Q^2 (> 3 GeV^2), a pQCD-inspired model involving GPDs has been proposed by Goloskokov and Kroll [8], in which the non-leading twist longitudinal double spin asymmetry results from the interference between the dominant GPD H_g and the helicity-dependent GPD $\tilde{H}_g$. The asymmetry is estimated to be of the order $k_T^2 \tilde{H}_g/(Q^2 H_g)$, where k_T is the transverse momentum of the quark and the antiquark.

The longitudinal double spin asymmetry A_1^ρ for the exclusive production of ρ^0 meson, $\mu + N \to \mu' + \rho^0 + N'$, has been measured by scattering longitudinally polarised muons off longitudinally polarised deuterons from the ^{6}LiD target and selecting incoherent exclusive ρ^0 production. The COMPASS results for 2002 and 2003 data [10] cover a wide kinematic range, $3 \cdot 10^{-3} \leq Q^2 \leq 7$ (GeV/c)^2 and $5 \cdot 10^{-5} \leq x \leq 0.05$. The measured asymmetry is shown as a function of Q^2 and x_{Bj} in Fig. 4. It is compatible with zero in the whole covered kinematic

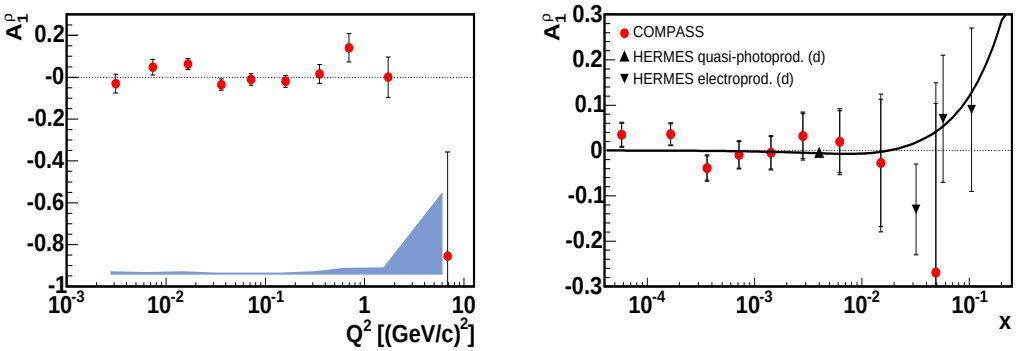

Figure 4: A_1^ρ as a function of Q^2 *(left)* and of x_{Bj} *(right)* from the present analysis compared to HERMES results on the deuteron target. The curve is described in the text.

range. This may indicate that the role of unnatural parity exchanges like π- or A_1-Reggeon exchange is small in that kinematic domain. The asymmetry is compared to HERMES results on the deuteron target [11]. The results from both experiments are consistent within errors. The kinematic range covered by the COMPASS measurements extends further towards small values of Q^2 and x_{Bj} by almost two orders of magnitude.

The x_{Bj} dependence of measured A_1^ρ is compared with the prediction $A_1^\rho = 2A_1/(1 + (A_1)^2)$ [12], which relates A_1^ρ with the A_1 asymmetry for inclusive inelastic lepton scattering at

the same x_{Bj}. The curve in Fig. 4 was obtained using the parameterisation of A_1 obtained from a fit [10] to the world data from polarised deuteron targets, including COMPASS measurements of A_1 at very low Q^2 and x_{Bj}. Within the present accuracy the results on A_1^ρ are consistent with this prediction.

5 Results for ρ^0 spin density matrix elements

Here we present preliminary results of the analysis of angular distributions for exclusive incoherent ρ^0 production $\mu + N \to \mu' + \rho^0 + N'$ and subsequent decay $\rho^0 \to \pi^+\pi^-$. The angular distributions allow one to determine ρ^0 spin density matrix elements (SDME) [13], which carry information on the spin structure of the production amplitudes. In particular, SDMEs allow one to test the s-channel helicity conservation (SCHC) and to determine $R = \sigma_L/\sigma_T$, the ratio of the longitudinal to transverse virtual photon cross section for $\gamma^* + N \to \rho^0 + N'$. The ρ^0 angular distribution $W(\cos\theta, \varphi, \phi)$ is studied in the s-channel helicity frame. The ρ^0 direction in the virtual photon-nucleon centre of mass system is taken as the quantization axis. The angle θ is the polar angle and φ the azimuthal angle of the positive decay meson in the ρ^0 centre of mass system. The angle φ is then that between the decay plane and the ρ^0 production plane (the γ^*-ρ^0 plane). The angle ϕ is that of the ρ^0 production plane with respect to the lepton scattering plane (cf. Sect. 3.1.).

The preliminary results presented here come from COMPASS 2002 data taken with the longitudinally polarised ^{6}LiD target. For the analysis of the spin density matrix elements the data with opposite target polarisations were merged resulting in the average target polarisation close to 0.

In this analysis we consider only single-dimensional projections of $W(\cos\theta, \varphi, \phi)$. For $\cos\theta$ and φ they are given by the following formulae

$$W(\cos\ \theta) = \frac{3}{4}[(1 - r^{04}_{00}) + (3\, r^{04}_{00} - 1)\cos^2\theta]\,, \tag{9}$$

$$W(\varphi) = \frac{1}{2\pi}[1 - 2r^{04}_{1-1}\cos 2\varphi + P_\mu\sqrt{1-\epsilon^2}\ 2\,\Im m\, r^3_{1-1}\sin 2\varphi]\,. \tag{10}$$

In above equations the r's are the spin density matrix elements for exclusive ρ^0 production, P_μ is the polarisation of muon beam and ϵ is the virtual photon polarisation parameter [13].

The element r^{04}_{00} is determined from $\cos\theta$ distribution, and can be interpreted as the fraction of longitudinal (helicity 0) ρ^0 in the sample. If SCHC holds, R can be obtained using

$$R = \frac{1}{(\epsilon + \delta)}\,\frac{r^{04}_{00}}{1 - r^{04}_{00}}\,, \tag{11}$$

where δ is the correction [13] to the ratio of the longitudinal and transverse virtual photon fluxes due to the finite lepton mass.

The COMPASS results on the Q^2 dependence of R are compared to other experiments in Fig. 5 (*left*). At small Q^2 the production by transverse photons (σ_T) dominates, while with increasing Q^2 the contribution of the production by longitudinal photons (σ_L) takes over at $Q^2 \simeq 2\,(\mathrm{GeV}/c)^2$.

From φ distribution one could determine two matrix elements r^{04}_{1-1} and $\Im m r^3_{1-1}$. COMPASS preliminary results are compared to other experiments in Fig. 5 (*right*). Note, that $\Im m\, r^3_{1-1}$ could be accessed only with polarised lepton beams. COMPASS measurements exhibit small

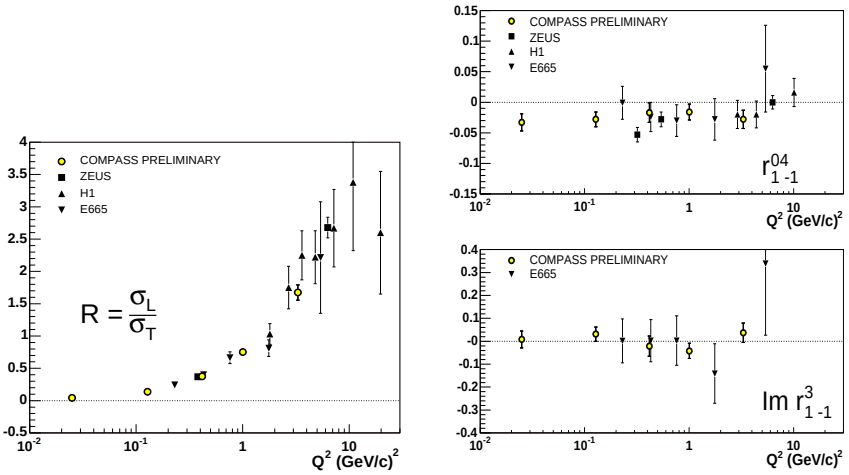

Figure 5: Q^2 dependence of $R = \sigma_L/\sigma_T$ (*left*) and of matrix elements r^{04}_{1-1} and $\Im m\, r^3_{1-1}$ (*right*)

negative values of r^{04}_{1-1} (≈ -0.03) approximately independent of Q^2, whereas $\Im m\, r^3_{1-1}$ is consistent with 0. The non-zero value of r^{04}_{1-1} indicates a small contribution of amplitudes with helicity flip.

In conclusion, the high precision COMPASS data on ρ^0 spin density matrix elements, which cover a wide range $0.01 < Q^2 < 10\ (\mathrm{GeV}/c)^2$, are consistent with a substantial increase of R with Q^2 and a weak violation of SCHC in agreement with other high energy experiments.

6 Future GPD program and 2008 DVCS test run

The study of GPDs using Deeply Virtual Compton Scattering and Hard Exclusive Meson Production is one of the topics proposed for the COMPASS future plans (COMPASS Phase II). The physics motivations are briefly described in a Letter of Intent [14] submitted to the CERN/SPSC in January 2009. A full proposal of the experiment will be submitted in 2009. The first stage of this program requires a 4 m long recoil detector (RPD) together with a 2.5 m long liquid hydrogen (LH) target. Upgrades of electromagnetic calorimeters to enlarge coverage at large x_{Bj} and reduce background are foreseen. The second stage requires a transversely polarised NH_3 target and a RPD.

The setup presently used for the meson spectroscopy measurements with hadron beams happens to be an excellent *prototype* to perform validation measurements for DVCS. A first measurements of exclusive γ production on a 40 cm long LH target, with detection of the slow recoiling proton in the RPD has been performed during a short (< 2 days) test run in 2008 using 160 GeV μ^+ and μ^- beams. The measurements were performed with the present hadron setup, all the standard COMPASS tracking detectors, the ECAL1 and ECAL2 electromagnetic calorimeters for photon detection and appropriate triggers. An efficient selection of single photon events, and suppression of the background is possible by using the combined information from the forward COMPASS detectors and the RPD.

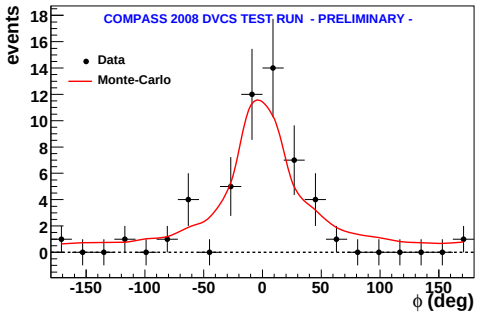

Figure 6: The distribution of the azimuthal angle ϕ for observed exclusive single photon production (points). The line is the Monte Carlo prediction normalised to the data.

A way to tag the observed process, $\mu + p \rightarrow \mu' + \gamma + p'$, to which both the DVCS and Bethe-Heitler process contribute, is to look at the angle ϕ between the leptonic and hadronic planes. The Bethe-Heitler contribution, which dominates the sample, show a peak at $\phi \simeq 0$. The observed distribution, after applying all cuts and selections and for $Q^2 > 1$ (GeV/c)^2, is displayed in Fig. 6 with the prediction from the Monte Carlo simulation. The shape of the observed distribution is compatible with the dominant Bethe-Heitler process. The overall detection efficiency can be deduced from the relative normalisation of the two distributions. The efficiency is equal to about 0.3.

7 Acknowledgments

This work was supported in part by Polish MSHE grant 41/N-CERN/2007/0.

References

[1] COMPASS Collab., P. Abbon *et al.*, Nucl. Instr. Meth. **A577** 455 (2007).
[2] K. Goeke, M.V. Polyakov, M. Vanderhaeghen, Prog. Part. in Nucl. Phys. **47** 401 (2001), hep-ph/0106012.
[3] F. Ellinghaus, W.-D. Nowak, A.V. Vinnikov, and Z. Ye, Eur. Phys. J. **C46** 729 (2006), hep-ph/0506264.
[4] X. Ji, Phys. Rev. Lett. **78** 610 (1997), hep-ph/9603249.
[5] M. Burkardt, Int. J. Mod. Phys. **A18** 173 (2003), hep-ph/0207047.
[6] M. Diehl and S. Sapeta, Eur. Phys. J. **C41** 515 (2005), hep-ph/0503023;
M. Diehl, JHEP 0709:064 (2007), hep-ph/0704.1565.
[7] HERMES Collab., A.Rostomyan *et al*, hep-ex/07072486 and DIF08, AIP Conf. Proc. 1105 (2009).
[8] S.V. Goloskokov, P. Kroll, Eur. Phys. J. **C42** 281 (2005), hep-ph/0501242;
S.V. Goloskokov, P. Kroll, Eur. Phys. J. **C53** 367 (2008), hep-ph/0708.3569;
[9] S.V. Goloskokov, P. Kroll, Eur. Phys. J. **C59** 809 (2009), hep-ph/0809.4126.
[10] COMPASS Collab., M. Alekseev *et al.*, Eur. Phys. J. **C 52** 255 (2007).
[11] HERMES Collab., A. Airapetian *et al.*, Eur. Phys. J. **C 29** 171 (2003).
[12] HERMES Collab., A. Airapetian *et al.*, Phys. Lett. **B 513** 301 (2001).
[13] K.Schilling and G.Wolf, Nucl.Phys. **B61** 381 (1973).
[14] COMPASS Collab., *COMPASS Medium and Long Term Plans*, CERN-SPSC-2009-003,SPSC-I-238.